Am J Physiol Cell Physiol 317: C358–C365, 2019.
First published June 5, 2019; doi:10.1152/ajpcell.00052.2019.

RESEARCH ARTICLE

A central core disease mutation in the Ca^{2+}-binding site of skeletal muscle ryanodine receptor impairs single-channel regulation

Venkat R. Chirasani,[1] Le Xu,[2] Hannah G. Addis,[3,4] Daniel A. Pasek,[2] Nikolay V. Dokholyan,[1] Gerhard Meissner,[2]* and Naohiro Yamaguchi[3,4]*

[1]*Departments of Pharmacology and Biochemistry and Molecular Biology, Penn State College of Medicine, Hershey, Pennsylvania;* [2]*Department of Biochemistry and Biophysics, University of North Carolina, Chapel Hill, North Carolina;* [3]*Department of Regenerative Medicine and Cell Biology, Medical University of South Carolina, Charleston, South Carolina; and* [4]*Cardiac Signaling Center of University of South Carolina, Medical University of South Carolina and Clemson University, Charleston, South Carolina*

Submitted 11 February 2019; accepted in final form 23 May 2019

Chirasani VR, Xu L, Addis HG, Pasek DA, Dokholyan NV, Meissner G, Yamaguchi N. A central core disease mutation in the Ca^{2+}-binding site of skeletal muscle ryanodine receptor impairs single-channel regulation. *Am J Physiol Cell Physiol* 317: C358–C365, 2019. First published June 5, 2019; doi:10.1152/ajpcell.00052.2019.—Cryoelectron microscopy and mutational analyses have shown that type 1 ryanodine receptor (RyR1) amino acid residues RyR1-E3893, -E3967, and -T5001 are critical for Ca^{2+}-mediated activation of skeletal muscle Ca^{2+} release channel. De novo missense mutation RyR1-Q3970K in the secondary binding sphere of Ca^{2+} was reported in association with central core disease (CCD) in a 2-yr-old boy. Here, we characterized recombinant RyR1-Q3970K mutant by cellular Ca^{2+} release measurements, single-channel recordings, and computational methods. Caffeine-induced Ca^{2+} release studies indicated that RyR1-Q3970K formed caffeine-sensitive, Ca^{2+}-conducting channel in HEK293 cells. However, in single-channel recordings, RyR1-Q3970K displayed low Ca^{2+}-dependent channel activity and greatly reduced activation by caffeine or ATP. A RyR1-Q3970E mutant corresponds to missense mutation RyR2-Q3925E associated with arrhythmogenic syndrome in cardiac muscle. RyR1-Q3970E also formed caffeine-induced Ca^{2+} release in HEK293 cells and exhibited low activity in the presence of the activating ligand Ca^{2+} but, in contrast to RyR1-Q3970K, was activated by ATP and caffeine in single-channel recordings. Computational analyses suggested distinct structural rearrangements in the secondary binding sphere of Ca^{2+} of the two mutants, whereas the interaction of Ca^{2+} with directly interacting RyR1 amino acid residues Glu^{3893}, Glu^{3967}, and Thr^{5001} was only minimally affected. We conclude that RyR1-Q3970 has a critical role in Ca^{2+}-dependent activation of RyR1 and that a missense RyR1-Q3970K mutant may give rise to myopathy in skeletal muscle.

central core disease; homology modeling; ryanodine receptor; sarcoplasmic reticulum; single-channel recording

INTRODUCTION

The skeletal muscle (RyR1) and cardiac muscle (RyR2) ryanodine receptor Ca^{2+} release channels are responsible for intracellular Ca^{2+} release from sarcoplasmic reticulum (SR) during muscle action potential. The RyRs are homotetramers of ~5,000 amino acid subunits that have multiple regulatory sites for physiological and pharmacological effectors (6, 13, 19). RyRs are activated by micromolar Ca^{2+} and millimolar ATP and caffeine and inhibited by millimolar Ca^{2+} and Mg^{2+}. Calcium release through RyRs is critical for skeletal and cardiac muscle contraction, and functional changes in the RyR protein complexes have been implicated in human pathologies. A large number of missense mutations are associated in RyR1 with malignant hyperthermia and central core disease (CCD) and are associated in RyR2 with catecholaminergic polymorphic ventricular tachycardia (10–12, 14, 30). Structural analyses of RyRs by crystallography and cryoelectron microscopy (cryo-EM) have provided detailed insights into RyR structural changes caused by disease-linked mutations and channel regulatory ligands (4, 5, 16, 24–26, 34–36).

The near-atomic resolution of the structure of purified RyR1 using cryo-EM and three-dimensional image analysis revealed binding sites for the three RyR1 channel agonists Ca^{2+}, ATP, and caffeine (4). The Ca^{2+}-binding site comprises amino acid residues Glu^{3893}, Glu^{3967}, and Thr^{5001} that directly interact with Ca^{2+} and residues His^{3895} and Gln^{3970} that are part of the secondary binding sphere of Ca^{2+}. Mutagenesis and single-channel recordings showed that the three amino acids directly interacting with Ca^{2+} play a critical role in Ca^{2+}-mediated activation of RyR1 (31). Single and double RyR1-E3893 and RyR1-E3967 mutants were not activated by Ca^{2+}, and RyR1-T5001 mutant reduced the apparent affinity for Ca^{2+}.

De novo CCD-linked mutation RyR1-Q3970K was identified in a 2-yr-old boy who was able to walk but not to run (28). Morphological analysis indicated few cores and focal loss of cross striations. Here, we tested the hypothesis that the CCD-associated RyR1-Q3970K mutant and RyR1-Q3970E mutant, corresponding to missense RyR2-Q3925E mutant, displayed an altered Ca^{2+}-dependent regulation. RyR2-Q3925E was reported to be associated with arrhythmogenic syndrome in cardiac muscle (18). Both RyR1-Q3970K and RyR1-Q3970E mutants formed caffeine-sensitive, Ca^{2+}-conducting channels in HEK293 cells and displayed low channel open probability in the presence of three RyR1-activating ligands, Ca^{2+}, ATP, and caffeine, in single-channel measurements. The results suggest that altered regulation of RyR1-Q3970K by Ca^{2+} and ATP

* G. Meissner and N. Yamaguchi contributed equally to this work.
Address for reprint requests and other correspondence: N. Yamaguchi, Dept. of Regenerative Medicine and Cell Biology, Medical Univ. of South Carolina, 173 Ashley Ave., MSC508, Charleston, SC 29425 (e-mail: yamaguch@musc.edu).

may give rise to skeletal muscle myopathy and imply that RyR2-Q3925E corresponding to RyR1-Q3970E is associated with cardiac muscle myopathy.

MATERIALS AND METHODS

Materials. Protease inhibitors were obtained from Sigma-Aldrich (St. Louis, MO), jetPRIME transfection reagent from Polyplus (New York, NY), and phospholipids from Avanti Polar Lipids (Alabaster, AL).

Preparation of mutant channels. Full-length rabbit RyR1 was cloned into the mammalian expression vector pCMV5 (8). Rabbit RyR1-Q3970K and -Q3970E mutations corresponding to human RyR1-Q3969 were introduced by the QuikChange site-directed mutagenesis method (Agilent, Santa Clara, CA) using *Pfu*-turbo DNA polymerase and mutagenic oligonucleotides (7). Amino acid numbering is described using the rabbit sequence (29). Wild-type (WT) and mutant RyR1s were transiently expressed in HEK293 cells using jetPRIME according to the manufacturer's instructions. Crude membrane isolates were prepared from the transfected HEK293 cells in the presence of protease inhibitors and 1 mM oxidized glutathione (GSSG) as described (33).

SDS-PAGE and immunoblot analysis. Proteins in crude membrane isolates of HEK293 cells (20 μg protein/lane) were separated using 3–12% gradient SDS-PAGE, transferred overnight to nitrocellulose membranes at 4°C, and probed using primary rabbit anti-RyR1 polyclonal antibody 6425, prepared by ψProSci (Poway, CA) (31). Immunoblots were developed using horseradish peroxidase-linked secondary anti-rabbit IgG antibody (Cell Signaling, Danvers, MA), and RyR1 proteins were quantified using Bio-Rad ChemiDoc MP Imaging System and ImageQuant TL analysis software.

Cellular Ca^{2+} release. Caffeine-induced Ca^{2+} release in HEK293 cells was measured using the fluorescence Ca^{2+} indicator Fluo-4. Briefly, HEK293 cells expressing wild-type (WT) or mutant RyR1s were grown on coverslips and incubated with membrane-permeable Fluo-4-AM (31). After washing away excess extracellular Fluo-4 AM, cellular Ca^{2+} release was triggered by the addition of ~8 mM caffeine and recorded in individual cells using Sola SEII Light Engine and NIS Elements Software (Nikon Instruments, Melville, NY). We probed nine coverslips for each genotype (WT, Q3970E, and Q3970K). On each coverslip, 30–50 cells were examined.

Single-channel recordings. Single-channel activities of WT and mutant RyR1s were recorded using the planar lipid bilayer method (31). Crude membrane isolates were added to the *cis* (cytosolic) chamber of a bilayer apparatus. Channel activities were measured using 0.25 M KCl and 20 mM K-HEPES, pH 7.4 on both sides of the bilayer, 2 μM *trans* (SR luminal) with indicated *cis* (cytosolic) Ca^{2+} concentrations and additions. The *trans* side of the bilayer was defined as ground. Electrical signals were filtered at 2 kHz, digitized at 10 kHz, and analyzed at 50% threshold setting (31). Data acquisition and analysis of 2-min recordings were performed using pClamp software (Molecular Devices, San Jose, CA).

Computational methods. The structures of the Ca^{2+}-binding site in RyR1-Q3970E and RyR1-Q3970K mutants were modeled by performing in silico amino acid substitutions in closed (PDB: 5TAQ) and open (PDB: 5TAL) RyR1-WT cryo-EM structures in the presence of Ca^{2+}, ATP, and caffeine. Prior to mutagenesis, the missing residues and atoms were relocated in both open and closed RyR1 structures through homology modeling. Subsequently, in silico mutations at chosen residue positions in RyR1 were performed using the Mutagenesis tool in PyMOL molecular visualization suite (https://pymol.org/2/) (3). During mutagenesis, the side-chain orientations of the substituted residues were selected based on *1*) backbone dependency and *2*) minimum clash score. The mutant RyR1 structures RyR1-Q3970E and RyR1-Q3970K were subjected to energy minimization by employing steepest descent and conjugate gradient algorithms in the GROMACS 4 package (9). Thus, generated optimal structures of RyR1-WT, RyR1-Q3970E, and RyR1-Q3970K in both closed and open conformations were analyzed and compared for loss/gain of interactions in Ca^{2+}-binding pocket, up to the second coordination sphere of Ca^{2+}, as described previously (31).

Biochemical assays and data analysis. Free Ca^{2+} concentrations were determined using a Ca^{2+}-selective electrode. Free Ca^{2+} concentrations following the addition of 2 mM ATP were calculated using MaxChelator (https://web.stanford.edu/~cpatton/downloads.htm) and constants from the Theo Schoenmakers' Chelator (27). Data are presented as the mean ± SE. Differences between samples were analyzed using ANOVA followed by Tukey's test, where $P < 0.05$ was considered significant.

RESULTS

In addition to three RyR1 amino acid residues (Glu^{3893}, Glu^{3967}, and Thr^{5001}) that directly bind Ca^{2+} (31), Gln^{3970} is part of the secondary coordination sphere of the Ca^{2+}-binding site conserved in RyR1 and RyR2 (Fig. 1) (4). To assess the significance of Gln^{3970} in Ca^{2+}-dependent activation of RyR1 in skeletal muscle central core disease pathology (28), we expressed RyR1-Q3970K in HEK293 cells and characterized recombinant mutant proteins by using a cellular Ca^{2+} release assay, single-channel recordings, and computational methods. We also prepared and characterized RyR1-Q3970E mutant, which corresponds to the RyR2-Q3925E mutant identified in a patient with arrhythmogenic syndrome (18). Some RyR1-WT data were previously published using the methods described in the present report (31).

Characterization RyR1-Q3970K and -Q3970E in HEK293 cells. Quantitative analysis of immunoblots showed specificity of the RyR1 polyclonal antibody for RyR1 (Fig. 2*A*, *left*). Protein levels of RyR1-Q3970E exceeded WT by 10- to 20-fold, whereas RyR1-Q3970K was twofold greater than WT (Fig. 2*A*, *right*). HEK293 cells expressing RyR1-E3893 or RyR1-E3967 also expressed at elevated levels compared with

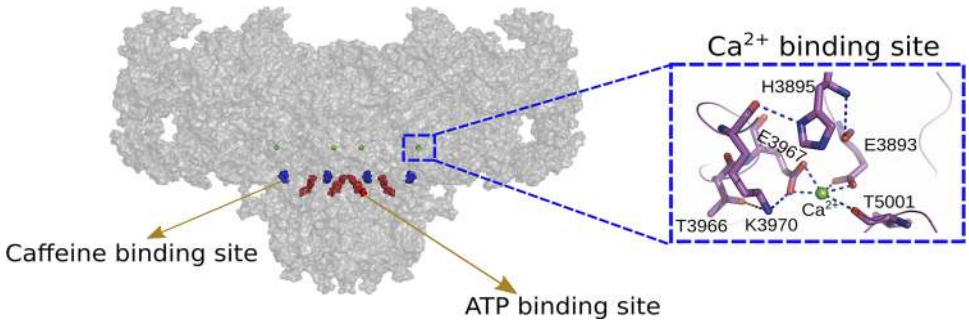

Fig. 1. Location of Ca^{2+}-, ATP-, and caffeine-binding sites of open type 1 ryanodine receptor-wild type (RyR1-WT; PDB code 5TAL). Protein structure is shown as a transparent surface. Ca^{2+}-, ATP-, and caffeine-binding sites are shown in green, red, and blue, respectively. *Inset*: structure of Ca^{2+}-binding site of open RyR1-Q3970K mutant in the presence of Ca^{2+}, ATP, and caffeine. [Modified from Xu et al. (31) with permission.]

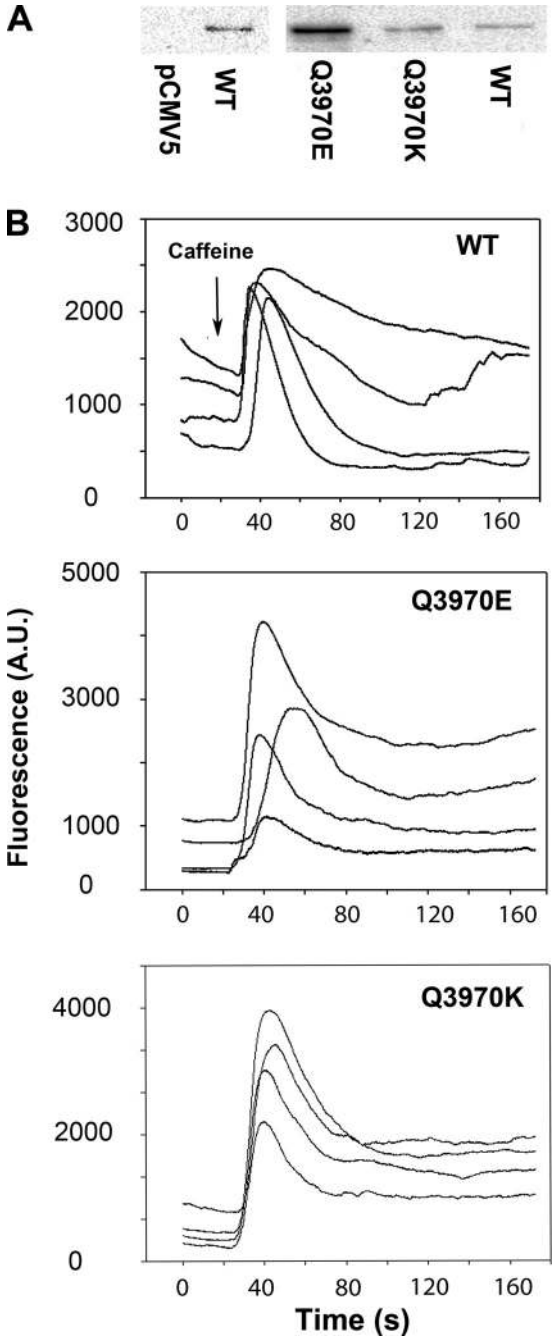

Fig. 2. Immunoblot and caffeine-induced Ca^{2+} release by HEK293 cells expressing wild-type (WT) and mutant type 1 ryanodine receptors (RyR1s). *A*: immunoblots of HEK293 cells transfected with pCMV5 vector and RyR1-WT expression vector (*left*), and 565 kDa RyR1-Q3970E, RyR1-Q3970K, and RyR1-WT (*right*). The blots identified the RyR1 protein band by its absence from the pCMV5 vector-transfected sample (*left*). *B*: Ca^{2+} transients in HEK293 cells expressing RyR1-WT (*top*), RyR1-Q3970E (*middle*), and RyR1-Q3970K (*bottom*) as changes of Fluo-4 fluorescence before and following the addition of 8 mM caffeine (arrow) to the bath solution. AU, arbitrary units.

WT (31). The functional expression of RyR1 mutants was determined using fluorescent Ca^{2+} indicator Fluo-4 and RyR1 agonist caffeine (Fig. 2*B*). Both RyR1-Q3970K and RyR1-Q3970E exhibited caffeine-dependent intracellular Ca^{2+} transients in intact HEK293 cells, indicating the expression of Ca^{2+}-conducting channels. A variable caffeine-induced Ca^{2+} release was observed in 40 ± 6% of HEK293 cells (n = 9) transfected with RyR1-WT. As previously reported (31), the variable response may have resulted from uneven exposure to caffeine and removal of released Ca^{2+} from the cells. The number of RyR1-Q3970E and RyR1-Q3970K cells responding to caffeine was significantly less than WT (12 ± 5%, n = 9, $P < 0.005$) and 14 ± 4%, n = 9, $P < 0.005$), respectively, despite the expression of elevated protein levels of both mutants compared with WT.

Single-channel analysis of mutant RyR1s. The lipid bilayer method was used to determine the regulation of RyR1-Q3970E and RyR1-Q3970K by endogenous activating ligands Ca^{2+} and ATP and exogenous ligand caffeine. Membrane isolates were fused with lipid bilayers, and single-channels were recorded using 0.25 M KCl on both sides of the bilayer, taking advantage of the impermeability of RyR1 to Cl^- and high permeability to K^+ compared with Ca^{2+}.

Single open-channel probability (P_o) of WT and mutant RyR1s was determined at various *cis* cytosolic Ca^{2+} concentrations. Figure 3 shows representative single-channel traces of RyR1-WT (Fig. 3*A*), RyR1-Q3970E (Fig. 3*B*), and RyR1-Q3970K (Fig. 3*C*) at cytosolic Ca^{2+} ranging from 0.01 μM to 1 mM. RyR1-WT exhibited a typical bimodal Ca^{2+}-dependent activation and inactivation profile with peak at ~20 μM Ca^{2+}, which indicated the presence of high-affinity Ca^{2+} activation and low-affinity Ca^{2+} inactivation sites (Fig. 3*D*). RyR1-Q3970E exhibited a low P_o compared with WT and shifted Ca^{2+} activation rightward. RyR1-Q3970K exhibited very low open probability (P_o) at all tested Ca^{2+} concentrations. A bimodal Ca^{2+} activation/inactivation profile comparable to WT suggested that the Q3970K mutation did not markedly alter RyR1 Ca^{2+} affinity at activation and inactivation sites (Fig. 3*D*, *inset*). The single-channel K^+ conductance for both mutants was essentially the same as for RyR1-WT (776 ± 17 pS, n = 8, for WT; 763 ± 7 pS, n = 7, for Q3970E; and 720 ± 23 pS, n = 4, for Q3970K; not shown).

Next, we tested whether mutant RyR1s can be activated by the two RyR agonists caffeine and ATP (19). To compare single-channel activities with the RyR1 structural models determined by cryo-EM, Ca^{2+}, caffeine, and ATP concentrations were used as reported by des Georges et al. (4). Single channels were recorded in the presence of 30 μM cytosolic Ca^{2+} at three different conditions: *1*) without caffeine or ATP, *2*) with 5 mM caffeine, and *3*) with 5 mM caffeine and 2 mM ATP (Fig. 4, *A–C*). In the presence of 5 mM caffeine, single-channel open probabilities of WT was 1.3-fold higher than Ca^{2+} only (average P_o were 0.20 and 0.26), and RyR1-Q3970E was 30-fold higher (P_o were 0.0003 and 0.009) (Fig. 4*D*). In the presence of both caffeine and ATP single-channel open probabilities of WT was 2.85-fold higher than 30 μM Ca^{2+} (P_o were 0.20 and 0.57), and RyR1-Q3970E was 123-fold (P_o were 0.0003 and 0.037). No significant difference in P_o was measured for RyR1-Q3970K in the presence of 5 mM caffeine or 5 mM caffeine and 2 mM ATP compared with 30 μM Ca^{2+} only.

DISCUSSION

High-resolution cryo-EM and structural analysis of intact RyR1 have shown that RyR1-Q3970 is part of a secondary coordination sphere of Ca^{2+}. De novo CCD-associated RyR1-

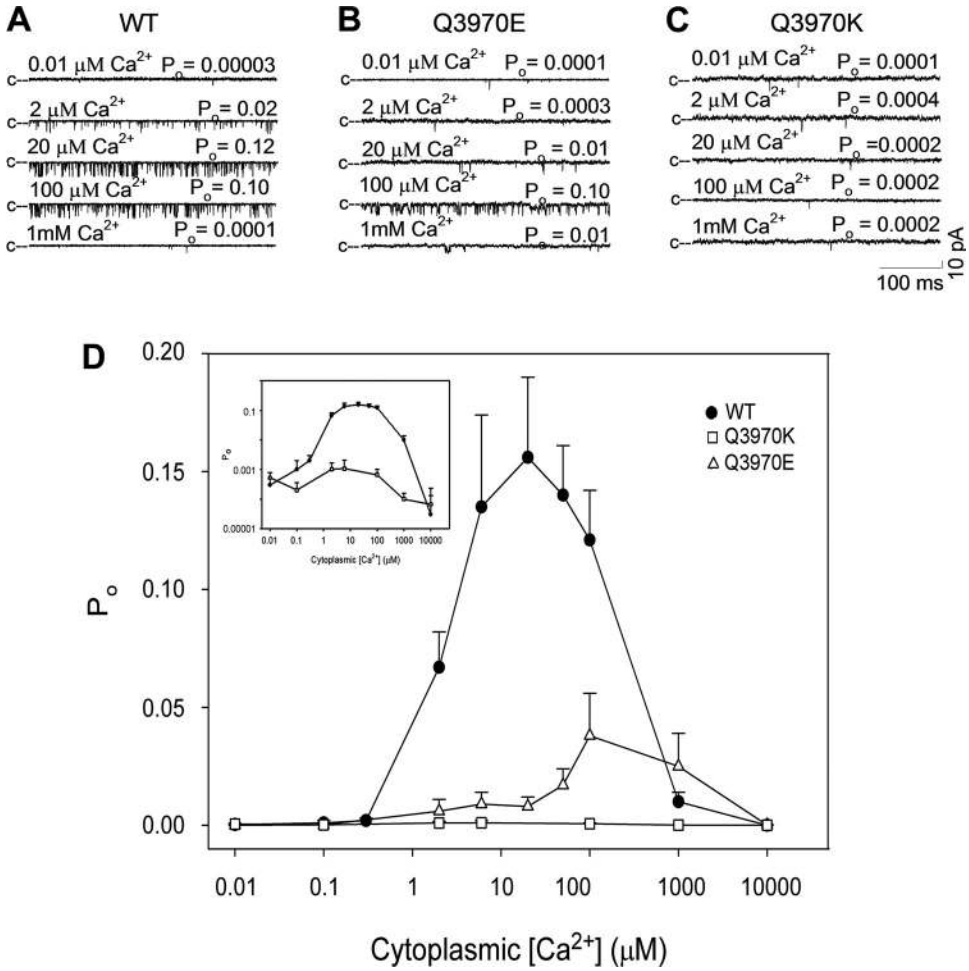

Fig. 3. Effects of cytosolic Ca^{2+} on type 1 ryanodine receptor-wild type (RyR1-WT) and mutant channel open probability (P_o). *A–C*: representative single-channel currents of RyR1-WT (*A*), RyR1-Q3970E (*B*), and RyR1-Q3970K (*C*) were recorded as downward deflections from the closed state (c–) in 250 mM symmetrical KCl at −20 mV with 2 μM sarcoplasmic reticulum (SR) luminal Ca^{2+} and the indicated cytosolic Ca^{2+} concentrations. *D*: Ca^{2+} dependence of RyR1-WT, RyR1-Q3970E, and RyR1-Q3970K channel open probabilities. Data are the mean ± SE of 3–21 recordings. *Inset*: open probabilities of WT and Q3970K in a logarithmic scale. [WT data in *D* were obtained from Xu et al. (31) under recording conditions used in the present report.]

Q3970K mutant exhibited a caffeine-induced Ca^{2+} response in HEK293 cells, indicating the expression of caffeine-sensitive, Ca^{2+}-conducting channels. In single-channel measurements, activation by Ca^{2+}, ATP, and caffeine was greatly reduced for RyR1-Q3970K compared with WT. This suggests that RyR1-Q3970K mutant channels underwent some structural changes outside the cellular environment or required cofactors lost during isolation. RyR1-Q3970E, which corresponds to RyR2-Q3925E associated with arrhythmogenic syndrome in cardiac muscle, also displayed a caffeine-induced Ca^{2+} release in HEK293 cells. RyR1-Q3970E was activated by Ca^{2+} with apparent reduced affinity and level of Ca^{2+} activation compared with WT. In contrast to RyR1-Q3970K, RyR1-Q3970E maintained ATP and caffeine activation. However, the maximal open probability of RyR1-Q3970E in the presence of all three activating ligands (Ca^{2+}, caffeine, and ATP) was ~15-fold lower than WT. Together, these findings suggest that the two mutants formed loss-of-function channels in lipid bilayers. Computational analysis of the two mutants suggested structural rearrangements in the secondary binding sphere of Ca^{2+}. On the other hand, both RyR1 mutations only minimally affected the interaction of Ca^{2+} with RyR1 amino acid residues Glu^{3893}, Glu^{3967}, and Thr^{5001} that directly interact with Ca^{2+} (Fig. 5).

Central core disease is a congenital skeletal muscle myopathy causing gradual muscle weakness after birth. In human pathology, large cores in the center of skeletal muscle lacking mitochondria and oxidative enzymes are observed (10). Thus far, over 60 missense mutations in the *RYR1* gene have been reported to be associated with CCD (21), and a number of human patients with these mutations are susceptible to malignant hyperthermia, another *RYR1*-linked skeletal myopathy. Using mutant RyR1 expressing dyspedic myotubes, two major types of RyR1 mutants were proposed to mediate CCD: *1*) leaky RyR1 channel causing SR Ca^{2+} store depletion, and *2*) loss-of-function RyR1 resulting in excitation-contraction "uncoupling". In both cases, reduced Ca^{2+} release through the mutant RyR1s caused muscle weakness (1, 2, 15).

Single-channel recordings have shown that CCD-associated RyR1 mutations affect channel function by causing loss-of-function ion conductances or gain-of-function gating activities. Ion conductance mutants result in low or absent Ca^{2+} conductance and are localized in the pore-forming carboxyl-terminal domain (I4897T, G4898E, G4898R, and ΔV4926-I4927 in rabbit RyR1 sequence), but also include amino terminal domain mutants (R110W and R110W/L486V in rabbit RyR1 sequence) (15, 17, 32, 37). Gating mutants have essentially the same single-channel Ca^{2+} conductance but display an open probability in single-channel recordings that results in "leaky" RyR1 channels and SR Ca^{2+} store depletion. Examples of gain-of-function mutants are CCD-linked RyR1-ΔR4215-F4217 (17), minicore myopathy mutant RyR1-N2283H (37),

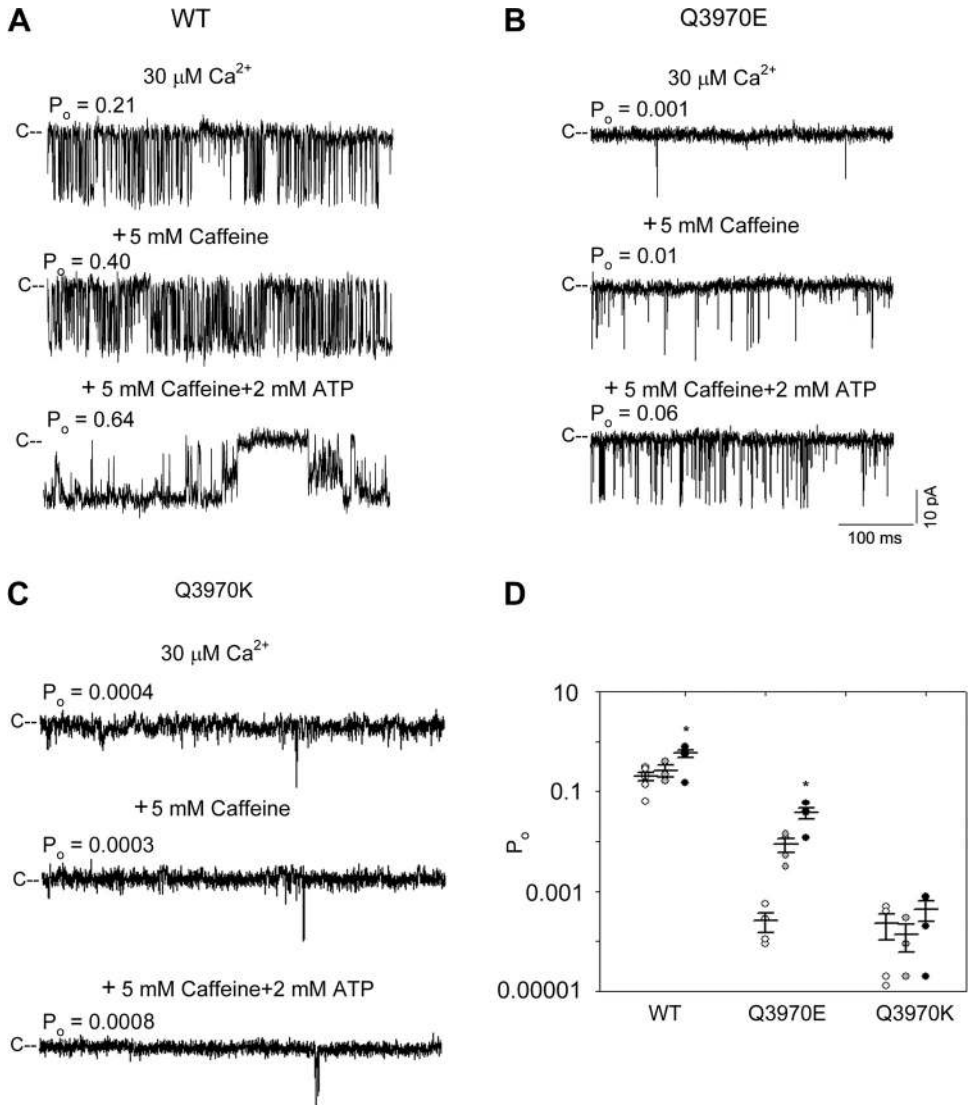

Fig. 4. Effects of caffeine and ATP on type 1 ryanodine receptor- wild type (RyR1-WT) and mutant channel open probabilities (P_o). *A–C*: representative single-channel currents of RyR1-WT (*A*), RyR1-Q3970E (*B*), and RyR1-Q3970K (*C*) were recorded as downward deflections from the closed state (C–) in 250 mM symmetrical KCl at −20 mV. Luminal Ca^{2+} was 2 μM. Cytosolic solutions contained 30 μM Ca^{2+} (*top traces*), 30 μM Ca^{2+} and 5 mM caffeine (*middle traces*), and 30 μM Ca^{2+}, 5 mM caffeine, and 2 mM ATP (*bottom traces*). Free Ca^{2+} was 5 μM in the presence of 5 mM caffeine and 2 mM ATP as described under MATERIALS AND METHODS. *D*: channel open probability in the presence of 30 μM cytoplasmic Ca^{2+} (open symbols), 30 μM Ca^{2+} and 5 mM caffeine (shaded symbols), and 5 μM Ca^{2+} plus 5 mM caffeine and 2 mM ATP (closed symbols). Data are the mean ± SE of 3–6 recordings. $*P < 0.05$ compared with respective controls by one-way ANOVA followed by Tukey's test. [WT data in *D* were obtained from Xu et al. (31) under recording conditions used in the present report.]

and likely RyR1-R164C and -Y523S, where the latter two exhibited leakiness of stored Ca^{2+} in skeletal myotubes or HEK293 cells (1, 21). RyR1-Q3970K appears to be a rare loss-of-function gating mutant. Recombinant homotetramer of RyR1-Q3970K conducted Ca^{2+} in HEK293 cells and, in contrast to conductance mutants (32), had a K^+ conductance comparable to that of WT in single-channel recordings. Ca^{2+} conductance and Ca^{2+}/K^+ permeability ratio could not be determined due to low open-channel probability of RyR1-Q3970K. The impact of the RyR1-Q3970K mutation on skeletal muscle excitation-contraction coupling may be further clarified by future knock-in mouse experiments. One possibility may be that the RyR1-Q3970K mutation will reduce the depolarization-induced Ca^{2+} release via an impaired secondary Ca^{2+}-induced Ca^{2+} release mechanism.

Using a [^{3}H]ryanodine ligand-binding assay, Murayama et al. (22) showed that, in the presence of 1 M NaCl, RyR2-Q3925E, which corresponds to RyR1-Q3970E, shifted the Ca^{2+} activation curve to the right without reducing maximal activity at millimolar Ca^{2+}. In our single-channel recordings, RyR1-Q3970E exhibited reduced affinity of Ca^{2+} activation and peak activity at 100 μM Ca^{2+} compared with WT at 20 μM Ca^{2+}. The differences in peak activities may have resulted from isoform-specific differences between skeletal and cardiac muscle RyRs and the high salt concentration used in the [^{3}H]ryanodine-binding assay. High salt concentrations are known to enhance RyR channel activity and levels of bound [^{3}H]ryanodine (20, 23). In addition, we found for the first time that RyR1-Q3970E maintained ATP and caffeine activation, although open probability of RyR1-Q3970E in the presence of three channel activators Ca^{2+}, ATP, and caffeine was low compared with WT. The impact of low open-channel probability on cardiac cellular Ca^{2+} signaling and the arrhythmogenic syndrome remain to be determined.

Our mutagenesis experiments have shown that glutamine substitution with lysine greatly reduced Ca^{2+}-mediated channel activity, and substitution with glutamate, carrying an opposite charge to lysine, decreased the apparent affinity of activating Ca^{2+}. Computational analysis using cryo-EM densities (4) determined the structure of the Ca^{2+}-binding sites of Ca^{2+}/ATP/caffeine-bound WT and mutant channels. In the closed RyR1-WT channel in the presence of activating

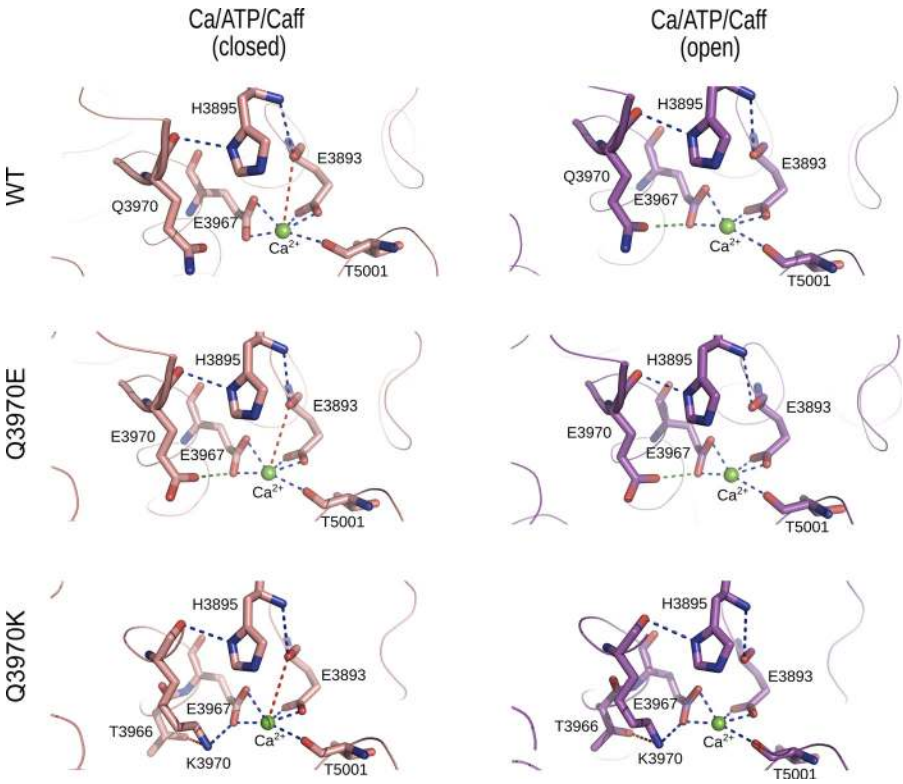

Fig. 5. Interactions of Ca^{2+} with wild type (WT) and mutant type 1 ryanodine receptors (RyR1s). Shown are predicted interactions of Ca^{2+} with WT and mutant RyR1s in the presence of Ca^{2+}, ATP, and caffeine. Residues displaying electrostatic interactions with Ca^{2+} in the Ca^{2+}/ATP/caffeine closed (5TAQ) and open (5TAL) states are depicted in stick representation. Backbone of RyR1 is shown as a ribbon. Ca^{2+} is shown as a green sphere. Strong electrostatic interactions (distance <3.2 Å) are shown as blue dashed lines and weak electrostatic interactions (distance <4 Å) are shown as red dashed lines between Ca^{2+} and RyR1 residues. Attractive and repulsive amino acid interactions (distance <3.5 Å) are depicted as blue and green dashed lines, respectively.

ligands Ca^{2+}, ATP, and caffeine, Gln^{3970} did not directly interact with Ca^{2+}, whereas Ca^{2+} strongly interacted with the side-chains of Glu^{3893}, Glu^{3967}, and Thr^{5001}. It is also apparent from the Ca^{2+}-binding site in Ca^{2+}/ATP/caffeine-bound closed WT and mutant channels that Ca^{2+} has weak interaction with the backbone carbonyl oxygen of Glu^{3893} (Fig. 5 and Table 1). Furthermore, our computational analysis indicated the presence of energetically favorable interactions between His^{3895} and Gln^{3970}, and between His^{3895} and Glu^{3893}. Rearrangements in the primary and secondary binding spheres of Ca^{2+} may have stabilized open WT channel states. These included loss of a weak interaction of Ca^{2+} with

Table 1. *Interactions between Ca^{2+} and amino acids of WT and mutant Ca^{2+} activation sites*

			Amino Acid Interactions				
Ca^{2+} Interactions	Class 5TAQ (Closed) Distance, Å	Class 5TAL (Open) Distance, Å	Class 5TAQ (Closed)	Distance, Å	Class 5TAL (Open)	Distance, Å	Type
WT variant							
E3893(OE1)	2.4	2.3	H3895(ND1) - Q3970(O)	3.0	H3895(ND1) - Q3970(O)	3.0	Attractive
E3893(OE2)	2.1	2.2	H3895(N) - E3893(O)	3.5	H3895(N) - E3893(O)	3.5	Attractive
E3893(O)	3.8				Q3970(OE1) - E3967(OE1)	3.3	Repulsive
E3967(OE1)	2.5	2.4					
E3967(OE2)	2.2	2.3					
T5001(O)	2.6	2.5					
Q3970E variant							
E3893(OE1)	2.4	2.3	H3895(ND1) - E3970(O)	3.0	H3895(ND1) - E3970(O)	3.0	Attractive
E3893(OE2)	2.1	2.2	H3895(N) - E3893(O)	3.5	H3895 (N) - E3893 (O)	3.5	Attractive
E3893(O)	3.8		E3970(OE1) - E3967(OE1)	3.3	E3970(OE1) - E3967(OE1)	3.0	Repulsive
E3967(OE1)	2.5	2.4					
E3967(OE2)	2.2	2.3					
T5001(O)	2.6	2.5					
Q3970K variant							
E3893(OE1)	2.4	2.3	K3970(NZ) - T3966(OG1)	3.9	K3970(NZ) - T3966(OG1)	3.8	Attractive
E3893(OE2)	2.1	2.2	K3970(NZ) - E3967(OE2)	2.9	K3970(NZ) - E3967(OE2)	2.6	Attractive
E3893(O)	3.8		K3970(O) - H3895(ND1)	3.0	K3970(O) - H3895(ND1)	3.0	Attractive
E3967(OE1)	2.5	2.4	H3895(N) - E3893(O)	3.5	H3895(N) - E3893(O)	3.5	Attractive
E3967(OE2)	2.2	2.3					
T5001(O)	2.6	2.5					

Strong electrostatic interactions (distance <3.5Å) are shown in Fig. 5 as blue dashed lines and weak electrostatic interactions (distance >3.5Å) are shown as red dashed lines between Ca^{2+} and type 1 ryanodine receptor (RyR1) residues. Distances less than 3.5Å formed between inter-residues in RyR1-Q3970K are shown as blue dashed lines; repulsive interactions are shown as green dotted lines. WT, wild type.

Glu^{3893} carbonyl oxygen and gain of repulsive interaction between Gln^{3970} and Glu^{3967} in open channel states.

In closed- and open-channel RyR1-Q3970E and RyR1-Q3970K structures, there were no marked changes in the interaction of Ca^{2+} with the side chains of Glu^{3893}, Glu^{3967}, and Thr^{5001} (Fig. 5 and Table 1). Neither the negatively charged glutamate in Q3970E nor the positively charged lysine in Q3970K directly interacted with Ca^{2+}. However, in RyR1-Q3970E, there occurred a repulsive interaction between two negatively charged Glu^{3970} and Glu^{3967}. Further, additional energetically favorable interactions formed by Lys^{3970} with its neighboring residues Thr^{3966} and Glu^{3967} were observed in RyR1-Q3970K (Fig. 5 and Table 1). These secondary structural changes and gain of interactions may be correlated to low channel activities as observed in RyR1-Q3970K single-channel recordings. Differences between the structural rearrangements in the Ca^{2+}-binding site of Q3970K and Q3970E variants are consistent with the different single-channel activities of the two RyR1 mutants.

Overall, our experimental and computational findings suggest that RyR1-Q3970K and RyR1-Q3970E did not alter channel activity by modifying the strong interactions of Ca^{2+} with Glu^{3893}, Glu^{3967}, and Thr^{5001} but rather by causing secondary structural changes in the presence of the three activating ligands Ca^{2+}, ATP, and caffeine. RyR1-Q3970 in the secondary coordination sphere of Ca^{2+} appears to be involved in Ca^{2+}-dependent activation of RyR1. Our data also suggest that RyR1-Q3970K is likely a CCD-associated loss-of-function channel that conducts Ca^{2+}, and functional characterization of this mutation in skeletal muscle will provide further insights into CCD pathology.

GRANTS

This study was supported by National Institutes of Health Grants GM-114015 and GM-123247 (to N. V. Dokholyan), AR-018687 (to G. Meissner), and P20 GM-103499 and UL1 TR-001450 (to N. Yamaguchi).

DISCLOSURES

No conflicts of interest, financial or otherwise, are declared by the authors.

AUTHOR CONTRIBUTIONS

G.M. and N.Y. conceived and designed research; V.R.C., L.X., H.G.A., D.A.P., and N.Y. performed experiments; V.R.C., L.X., H.G.A., D.A.P., N.V.D., G.M., and N.Y. analyzed data; V.R.C., L.X., H.G.A., D.A.P., N.V.D., G.M., and N.Y. interpreted results of experiments; V.R.C., L.X., and G.M. prepared figures; G.M. and N.Y. drafted manuscript; V.R.C., L.X., H.G.A., D.A.P., N.V.D., G.M., and N.Y. edited and revised manuscript; V.R.C., L.X., H.G.A., D.A.P., N.V.D., G.M., and N.Y. approved final version of manuscript.

REFERENCES

1. **Avila G, Dirksen RT.** Functional effects of central core disease mutations in the cytoplasmic region of the skeletal muscle ryanodine receptor. *J Gen Physiol* 118: 277–290, 2001. doi:10.1085/jgp.118.3.277.
2. **Avila G, O'Brien JJ, Dirksen RT.** Excitation-contraction uncoupling by a human central core disease mutation in the ryanodine receptor. *Proc Natl Acad Sci USA* 98: 4215–4220, 2001. doi:10.1073/pnas.071048198.
3. **DeLano WL.** *The PyMOL Molecular Graphics System, version 1.5.0.4*. New York: Schrödinger, 2011. https://pymol.org/2/.
4. **des Georges A, Clarke OB, Zalk R, Yuan Q, Condon KJ, Grassucci RA, Hendrickson WA, Marks AR, Frank J.** Structural basis for gating and activation of RyR1. *Cell* 167: 145–157.e17, 2016. doi:10.1016/j.cell.2016.08.075.
5. **Efremov RG, Leitner A, Aebersold R, Raunser S.** Architecture and conformational switch mechanism of the ryanodine receptor. *Nature* 517: 39–43, 2015. doi:10.1038/nature13916.
6. **Franzini-Armstrong C, Protasi F.** Ryanodine receptors of striated muscles: a complex channel capable of multiple interactions. *Physiol Rev* 77: 699–729, 1997. doi:10.1152/physrev.1997.77.3.699.
7. **Gao L, Balshaw D, Xu L, Tripathy A, Xin C, Meissner G.** Evidence for a role of the lumenal M3-M4 loop in skeletal muscle Ca^{2+} release channel (ryanodine receptor) activity and conductance. *Biophys J* 79: 828–840, 2000. doi:10.1016/S0006-3495(00)76339-9.
8. **Gao L, Tripathy A, Lu X, Meissner G.** Evidence for a role of C-terminal amino acid residues in skeletal muscle Ca^{2+} release channel (ryanodine receptor) function. *FEBS Lett* 412: 223–226, 1997. doi:10.1016/S0014-5793(97)00781-3.
9. **Hess B, Kutzner C, van der Spoel D, Lindahl E.** GROMACS 4: algorithms for highly efficient, load-balanced, and scalable molecular simulation. *J Chem Theory Comput* 4: 435–447, 2008. doi:10.1021/ct700301q.
10. **Jungbluth H, Treves S, Zorzato F, Sarkozy A, Ochala J, Sewry C, Phadke R, Gautel M, Muntoni F.** Congenital myopathies: disorders of excitation-contraction coupling and muscle contraction. *Nat Rev Neurol* 14: 151–167, 2018. doi:10.1038/nrneurol.2017.191.
11. **Landstrom AP, Dobrev D, Wehrens XH.** Calcium signaling and cardiac arrhythmias. *Circ Res* 120: 1969–1993, 2017. doi:10.1161/CIRCRESAHA.117.310083.
12. **Lanner JT.** Ryanodine receptor physiology and its role in disease. *Adv Exp Med Biol* 740: 217–234, 2012. doi:10.1007/978-94-007-2888-2_9.
13. **Lanner JT, Georgiou DK, Joshi AD, Hamilton SL.** Ryanodine receptors: structure, expression, molecular details, and function in calcium release. *Cold Spring Harb Perspect Biol* 2: a003996, 2010. doi:10.1101/cshperspect.a003996.
14. **Leenhardt A, Denjoy I, Guicheney P.** Catecholaminergic polymorphic ventricular tachycardia. *Circ Arrhythm Electrophysiol* 5: 1044–1052, 2012. doi:10.1161/CIRCEP.111.962027.
15. **Loy RE, Orynbayev M, Xu L, Andronache Z, Apostol S, Zvaritch E, MacLennan DH, Meissner G, Melzer W, Dirksen RT.** Muscle weakness in *Ryr1*$^{I4895T/WT}$ knock-in mice as a result of reduced ryanodine receptor Ca^{2+} ion permeation and release from the sarcoplasmic reticulum. *J Gen Physiol* 137: 43–57, 2011. doi:10.1085/jgp.201010523.
16. **Ludtke SJ, Serysheva II, Hamilton SL, Chiu W.** The pore structure of the closed RyR1 channel. *Structure* 13: 1203–1211, 2005. doi:10.1016/j.str.2005.06.005.
17. **Lyfenko AD, Ducreux S, Wang Y, Xu L, Zorzato F, Ferreiro A, Meissner G, Treves S, Dirksen RT.** Two central core disease (CCD) deletions in the C-terminal region of RYR1 alter muscle excitation-contraction (EC) coupling by distinct mechanisms. *Hum Mutat* 28: 61–68, 2007. doi:10.1002/humu.20409.
18. **Medeiros-Domingo A, Bhuiyan ZA, Tester DJ, Hofman N, Bikker H, van Tintelen JP, Mannens MM, Wilde AA, Ackerman MJ.** The RYR2-encoded ryanodine receptor/calcium release channel in patients diagnosed previously with either catecholaminergic polymorphic ventricular tachycardia or genotype negative, exercise-induced long QT syndrome: a comprehensive open reading frame mutational analysis. *J Am Coll Cardiol* 54: 2065–2074, 2009. doi:10.1016/j.jacc.2009.08.022.
19. **Meissner G.** The structural basis of ryanodine receptor ion channel function. *J Gen Physiol* 149: 1065–1089, 2017. doi:10.1085/jgp.201711878.
20. **Meissner G, Rios E, Tripathy A, Pasek DA.** Regulation of skeletal muscle Ca^{2+} release channel (ryanodine receptor) by Ca^{2+} and monovalent cations and anions. *J Biol Chem* 272: 1628–1638, 1997. doi:10.1074/jbc.272.3.1628.
21. **Murayama T, Kurebayashi N, Yamazawa T, Oyamada H, Suzuki J, Kanemaru K, Oguchi K, Iino M, Sakurai T.** Divergent activity profiles of type 1 ryanodine receptor channels carrying malignant hyperthermia and central core disease mutations in the amino-terminal region. *PLoS One* 10: e0130606, 2015. doi:10.1371/journal.pone.0130606.
22. **Murayama T, Ogawa H, Kurebayashi N, Ohno S, Horie M, Sakurai T.** A tryptophan residue in the caffeine-binding site of the ryanodine receptor regulates Ca^{2+} sensitivity. *Commun Biol* 1: 98, 2018. doi:10.1038/s42003-018-0103-x.
23. **Ogawa Y, Harafuji H.** Osmolarity-dependent characteristics of [^{3}H]ryanodine binding to sarcoplasmic reticulum. *J Biochem* 107: 894–898, 1990. doi:10.1093/oxfordjournals.jbchem.a123144.
24. **Peng W, Shen H, Wu J, Guo W, Pan X, Wang R, Chen SR, Yan N.** Structural basis for the gating mechanism of the type 2 ryanodine receptor RyR2. *Science* 354: aah5324, 2016. doi:10.1126/science.aah5324.

25. **Samsó M, Feng W, Pessah IN, Allen PD.** Coordinated movement of cytoplasmic and transmembrane domains of RyR1 upon gating. *PLoS Biol* 7: e85, 2009. doi:10.1371/journal.pbio.1000085.
26. **Samsó M, Wagenknecht T, Allen PD.** Internal structure and visualization of transmembrane domains of the RyR1 calcium release channel by cryo-EM. *Nat Struct Mol Biol* 12: 539–544, 2005. doi:10.1038/nsmb938.
27. **Schoenmakers TJ, Visser GJ, Flik G, Theuvenet AP.** CHELATOR: an improved method for computing metal ion concentrations in physiological solutions. *Biotechniques* 12: 870–874, 1992.
28. **Snoeck M, van Engelen BG, Küsters B, Lammens M, Meijer R, Molenaar JP, Raaphorst J, Verschuuren-Bemelmans CC, Straathof CS, Sie LT, de Coo IF, van der Pol WL, de Visser M, Scheffer H, Treves S, Jungbluth H, Voermans NC, Kamsteeg EJ.** RYR1-related myopathies: a wide spectrum of phenotypes throughout life. *Eur J Neurol* 22: 1094–1112, 2015. doi:10.1111/ene.12713.
29. **Takeshima H, Nishimura S, Matsumoto T, Ishida H, Kangawa K, Minamino N, Matsuo H, Ueda M, Hanaoka M, Hirose T, Numa S.** Primary structure and expression from complementary DNA of skeletal muscle ryanodine receptor. *Nature* 339: 439–445, 1989. doi:10.1038/339439a0.
30. **Treves S, Jungbluth H, Muntoni F, Zorzato F.** Congenital muscle disorders with cores: the ryanodine receptor calcium channel paradigm. *Curr Opin Pharmacol* 8: 319–326, 2008. doi:10.1016/j.coph.2008.01.005.
31. **Xu L, Chirasani VR, Carter JS, Pasek DA, Dokholyan NV, Yamaguchi N, Meissner G.** Ca^{2+}-mediated activation of the skeletal-muscle ryanodine receptor ion channel. *J Biol Chem* 293: 19501–19509, 2018. doi:10.1074/jbc.RA118.004453.
32. **Xu L, Wang Y, Yamaguchi N, Pasek DA, Meissner G.** Single-channel properties of heterotetrameric mutant RyR1 ion channels linked to core myopathies. *J Biol Chem* 283: 6321–6329, 2008. doi:10.1074/jbc.M707353200.
33. **Yamaguchi N, Xu L, Pasek DA, Evans KE, Meissner G.** Molecular basis of calmodulin binding to cardiac muscle Ca^{2+} release channel (ryanodine receptor). *J Biol Chem* 278: 23480–23486, 2003. doi:10.1074/jbc.M301125200.
34. **Yan Z, Bai X, Yan C, Wu J, Li Z, Xie T, Peng W, Yin C, Li X, Scheres SHW, Shi Y, Yan N.** Structure of the rabbit ryanodine receptor RyR1 at near-atomic resolution. *Nature* 517: 50–55, 2015. doi:10.1038/nature14063.
35. **Yuchi Z, Van Petegem F.** Ryanodine receptors under the magnifying lens: Insights and limitations of cryo-electron microscopy and X-ray crystallography studies. *Cell Calcium* 59: 209–227, 2016. doi:10.1016/j.ceca.2016.04.003.
36. **Zalk R, Clarke OB, des Georges A, Grassucci RA, Reiken S, Mancia F, Hendrickson WA, Frank J, Marks AR.** Structure of a mammalian ryanodine receptor. *Nature* 517: 44–49, 2015. doi:10.1038/nature13950.
37. **Zhou H, Yamaguchi N, Xu L, Wang Y, Sewry C, Jungbluth H, Zorzato F, Bertini E, Muntoni F, Meissner G, Treves S.** Characterization of recessive RYR1 mutations in core myopathies. *Hum Mol Genet* 15: 2791–2803, 2006. doi:10.1093/hmg/ddl221.